

# A 2.5 W LDMOS MICROWAVE TOTEM-POLE PUSH-PULL RF POWER AMPLIFIER

Gavin T. Watkins

Toshiba Research Europe Limited, 32 Queen Square, Bristol, BS1 4ND, UK  
Gavin.watkins@toshiba-trel.com

*RF push-pull power amplifiers (PA) typically use a transformer or balun at the output to combine the two anti-phase signals. The push-pull PA described here uses a totem-pole output stage consisting of two N-channel FETs; a source-follower to supply current to a 50  $\Omega$  load, and a common-source amplifier to sink current. The source tab of the source-follower cannot be grounded to dissipate heat in the normal way, so a ceramic spacer transfers the heat to an aluminum heatsink with minimum stray parasitic components.*

*A prototype PA was designed for 700 MHz. Under continuous wave (CW) excitation, it achieved a 1 dB compression point ( $P_{1dB}$ ) of 33.9 dBm (2.46 W) at an efficiency of 46.5%. The second harmonic distortion ( $HD_2$ ) suppression was 43.6 dB relative to the fundamental. These results indicate that the PA was operating in a push-pull mode.*

## INTRODUCTION

Push-pull RF PAs generally consist of two identical single ended amplifiers operate in anti-phase, with one amplifying the positive signal excursion, and the other the negative excursions. Anti-phase splitting and combining networks based on: wound transformers [1], or baluns [2] [3] are needed at the input and output, which can take up significant board space. The RF Energy Alliance predict that PA volume will shrink by up to 80% in the future [4]. This reduction in size is only possible without transformers and baluns.

At low frequencies both positive (i.e. N-channel FETs and NPN bipolar transistors) and negative (i.e. P-channel FETs and PNP bipolar transistors) polarity device are available. These are often available in complementary pairs making the push pull amplifier shown in Fig. 1 (a) possible, where  $Q_3$  is an NPN transistor and  $Q_4$  a PNP.

At microwave frequencies, performance of negative devices degrades [5] so the transformer coupled push-pull amplifier shown in Fig. 1 (b) is common. This amplifier uses two NPN bipolar transistors ( $Q_5$  and  $Q_6$ ) or two N-channel FET.

A transformer free alternative is the totem-pole amplifier based on two positive polarity devices ( $Q_7$  and  $Q_8$ ) as shown in Fig. 1 (c). This has been demonstrated at low RF frequencies with both active input drivers [6] and transformers [7] for the upper FET. A broadband bipolar MMIC

totem-pole amplifier with an active input driver for VHF was described in Reference [8], but resulted in a low efficiency of 14% at 100 MHz with 20 dBm (100 mW) output power ( $P_{OUT}$ ).

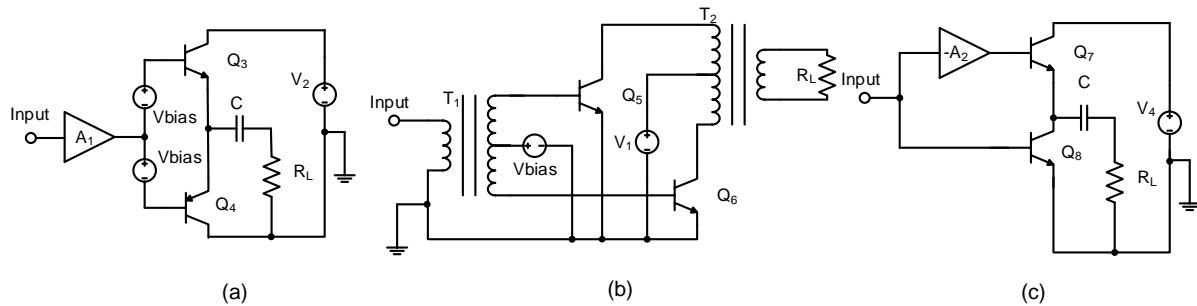


Fig. 1. Push-pull amplifier schematics (a) complementary bipolar, (b) transformer coupled and (c) totem pole

The totem-pole push-pull amplifier in this work is different to that previously described in the literature [6] [7] since it uses a reactive matching network at the input of the upper device. Previous work with GaAs devices [9] has produced a 230 mW  $P_{OUT}$  PA. Here,  $P_{OUT}$  is increased to 2.46 W with LDMOS devices.

## TOTEM-POLE PUSH-PULL AMPLIFIER

The complete schematic for an N-channel based totem-pole push-pull amplifier is shown in Fig. 2. The RF input signal is first split with a Wilkinson power splitter and the resulting output signals gain and phase aligned before applying to the active devices ( $Q_1$  and  $Q_2$ ), so that they operate in anti-phase.  $Q_2$  is a common source amplifier for sinking current from the 50  $\Omega$  load and  $Q_1$  is the source follower to supply current to the load. Variable Resistors  $R_1$  and  $R_2$  set a class B bias.

The low input impedance of  $Q_2$  is matched to 50  $\Omega$  with  $C_2$  and  $L_2$ . The input impedance of  $Q_1$  is low relative to its source terminal, but high when referenced to ground. Input matching is with  $C_1$  and  $L_1$ , which form a voltage step-up network. Source-followers have slightly less than unity voltage gain, but because of their high input impedance, have a large current gain. When the voltage step-up nature of  $C_1$  and  $L_1$  is combined with the high current gain of  $Q_1$ , overall power gain is achieved.

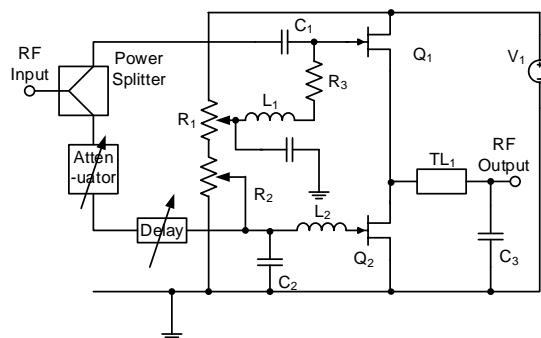


Fig. 2. Totem-pole amplifier schematic

$Q_1$ 's input impedance relative to ground ( $Z_i$ ) is a function of its common-source input impedance ( $Z_{i1}$ ), the load presented to its source ( $Z_L$ ) by the matching network formed by transmission line  $TL_1$  and  $C_3$ , and its transconductance ( $g_m$ ):

$$Z_i = Z_{i1} \cdot (2 \cdot Z_L \cdot g_m + 1) \quad (1)$$

It is assumed that  $Q_1$  and  $Q_2$  are the same device, although this does not necessarily have to be true. Resistor  $R_3$  improves stability since feedback can occur through  $Q_1$ 's gate-source capacitance ( $C_{gs}$ ).

Since the two halves of the amplifier are asymmetric, their phase shifts will be different. The Delay element in Fig. 2 is adjusted for correct push-pull operation. To suppress the  $HD_2$ , the gain of the two halves must also be matched, a variable attenuator performs this task.

## SOURCE-FOLLOWER COOLING

High power RF transistors are generally bolted or soldered to a heatsink via their source terminal to dissipate excess heat. In a totem-pole PA,  $Q_1$ 's source carries an RF signal, so cannot be. It must however still be thermally connected to the heatsink, but not electrically. The amplifier described in Ref. [10] used alumina insulators between the active devices and a heatsink. Here, a MPC101020T ceramic insulator from Amec Thermasol transfers the heat dissipated by an LDMOS PD85004 RF power transistor to the heatsink. To ensure minimum stray capacitance a nylon block clamps  $Q_1$  to the ceramic insulator and in-turn to the aluminium heatsink as shown in Fig. 3 (a). Thermal paste is used between all contacting surfaces.

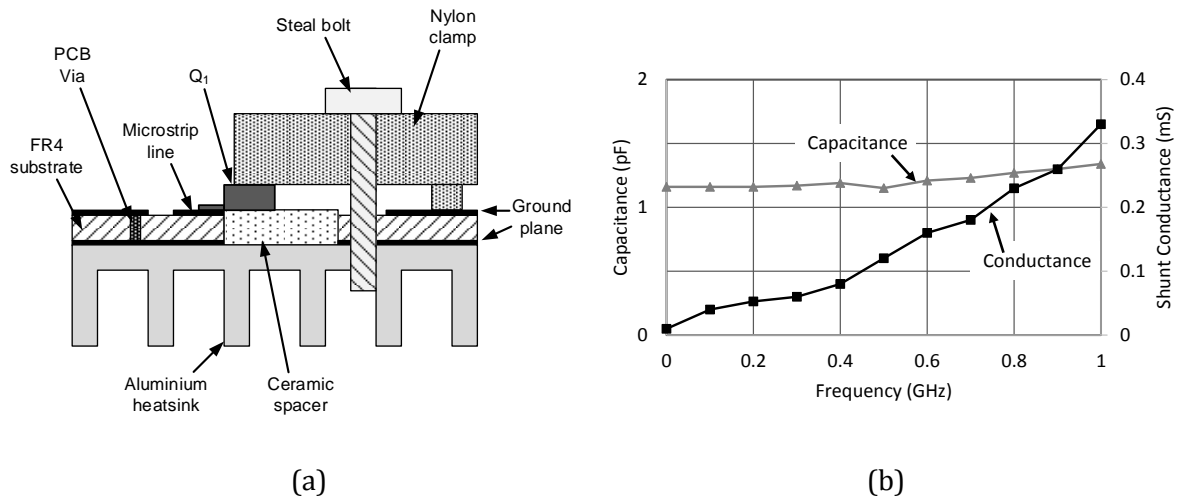


Fig. 3. (a) Mechanical arrangement of heatsink, (b) capacitance and shunt conductance of ceramic spacer

The junction temperature ( $T_j$ ) of  $Q_1$  must not exceed  $150^\circ\text{C}$ . Assuming an ambient room temperature ( $T_{amb}$ ) of  $25^\circ\text{C}$ , the maximum temperature rise ( $\Delta T$ ) is  $125^\circ\text{C}$  [11]:

$$\Delta T = T_j - T_{amb} \quad \Delta T = T_j - T_{amb} \quad (2)$$

The maximum power dissipation ( $P_{diss}$ ) for  $Q_1$  can be calculated:

$$P_{diss} = \frac{\Delta T}{\theta_{total}} \quad (3)$$

Where  $\theta_{total}$  is the total thermal resistance from  $Q_1$ 's junction to free space:

$$\theta_{total} = \theta_{jc} + \theta_{cs} + \theta_{sa} \quad (4)$$

The ceramic insulator had a thermal resistance of  $10.2 \text{ }^\circ\text{C/W}$  ( $\theta_{cs}$ ), and the heatsink  $3 \text{ }^\circ\text{C/W}$  to ambient ( $\theta_{sa}$ ). These are both less than the  $21 \text{ }^\circ\text{C/W}$  junction-to-case thermal resistance ( $\theta_{jc}$ ) of the PD85004. Therefore  $\theta_{total}$  is  $34.2 \text{ }^\circ\text{C/W}$ .  $\theta_{total}$  for  $Q_2$  will be different since it dissipates its heat through PCB vias, which can also be calculated [12].

A stray capacitor is formed by the source terminal of  $Q_1$ , ceramic insulator and heatsink. In reference [10] this stray capacitance was  $8 \text{ pF}$ . The capacitance here was measured as  $1.2 \text{ pF}$  by attaching pieces of copper tape to each side of the ceramic spacer. One side completely covered the spacer to represent the ground plane, and the other was approximately the same size as the source tab. By measuring the  $S_{11}$  with a vector network analyser, the capacitance and conductance was calculated. The capacitance is reasonably flat as shown in Fig. 3 (b), while the conductance at  $700 \text{ MHz}$  was  $0.2 \text{ mS}$ . Both are low enough to have a negligible effect.

## AMPLIFIER DESIGN

The amplifier was constructed on a single sided FR4 substrate with ground plane as shown in Fig. 4. A hole was cut to accommodate the ceramic insulator, as indicated in Fig. 3 (a). A resistive attenuator pad was included in one branch of Wilkinson splitter for gain alignment. Phase alignment was with calibrated lengths of cable and SMA adapters.

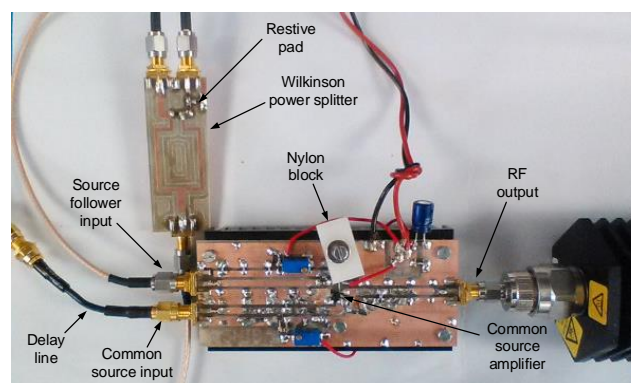


Fig. 4. Photograph of amplifier

Using the datasheet as a guide, the input and output matching networks were calculated. An optimum  $Z_L$  of  $6.3 + 1.7j \ \Omega$  was found and  $Z_{11}$   $17.4 - 29.6j \ \Omega$  at the operating frequency of  $700 \text{ MHz}$ . The  $g_m$  from the datasheet was  $0.75$ , resulting in a  $Z_1$  of  $257 - 267j \ \Omega$ .  $R_3$  was chosen as  $360 \ \Omega$ , reducing the source-follower input impedance to  $183 - 77j \ \Omega$ .

## PRACTICAL RESULTS

With a CW signal applied to the PA, the gain and phase imbalance between the two paths were set to a given value and input power swept.  $P_{OUT}$ , efficiency and  $HD_2$  suppression were recorded. The  $P_{1dB}$  sweep is shown in Fig. 5 (a). The efficiency and  $HD_2$  suppressions had similar profiles as shown in Fig. 5 (b) and Fig. 5 (c) respectively.

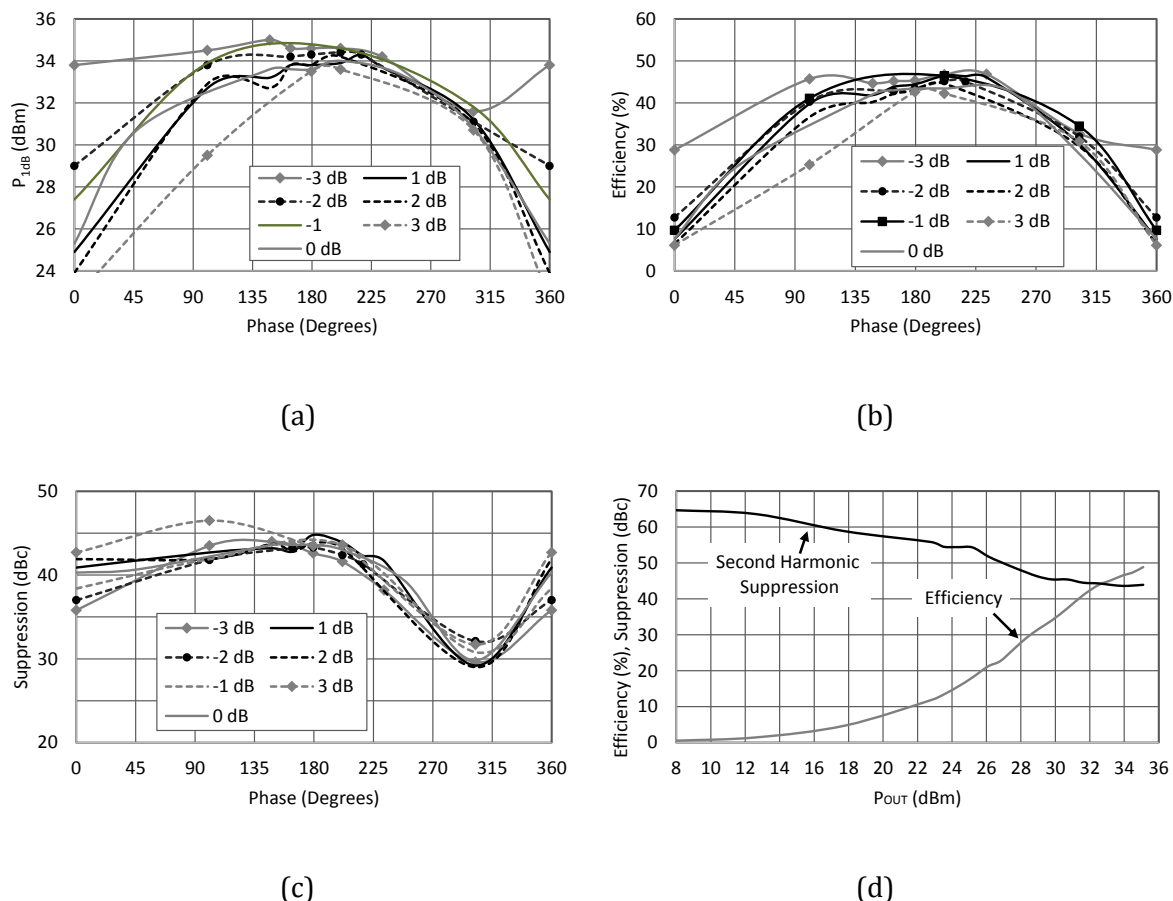


Fig. 5. (a)  $P_{1dB}$ , (b) efficiency and (c)  $HD_2$  at the  $P_{1dB}$  verse gain and phase imbalance. (d) Power sweep at optimum gain and phase setting

In Fig. 5 (a), (b) and (c), a negative gain indicates attenuation in the common-source path and a positive the source-follower. The optimum gain and phase imbalance were determined to be -1 dB and  $148^\circ$  respectively, resulting in a  $P_{1dB}$  of 33.9 dBm (2.46 W) and efficiency of 46.5%. Therefore the total PA power dissipation was 2.82W, resulting in a  $Q_1 P_{diss}$  of 1.42 W. Using (2) and (3),  $\Delta T$  was  $48.4^\circ\text{C}$  and  $T_j$   $73.4^\circ\text{C}$ , well below the  $150^\circ\text{C}$  maximum. The  $HD_2$  suppression was 43.6 dBc relative to the fundamental. A sweep of efficiency and  $HD_2$  suppression against  $P_{OUT}$  is shown in Fig. 5 (d). There is very little comparable research, but it is compared to closest published work in Table 1.

Table 1: Comparison of totem-pole amplifiers with CW signal

| Reference | Measurement Frequency (MHz) | $P_{OUT}$ (W) | Efficiency (%) |
|-----------|-----------------------------|---------------|----------------|
| [5]       | 8000                        | 0.01          | 20             |
| [6]       | 1                           | 3.7           | 58.3           |
| [7]       | 1-30                        | 560*          | 77.0*          |
| [8]       | 100                         | 0.1           | 14.0           |
| [9]       | 680                         | 0.23          | 52.0           |
| This Work | 700                         | 2.46          | 46.5           |

\*estimated from modulated results

## CONCLUSION

A totem-pole RF PA is described composed of common-source and source-follower amplifiers. A ceramic insulator transfers dissipated heat from the source-follower to a heatsink. When correctly aligned 46.5% efficiency was achieved at 33.9 dBm  $P_{OUT}$ . Under these conditions the  $HD_2$  suppression was 43.6 dBc relative to the fundamental output signal. The high efficiency and  $HD_2$  suppression indicate that this amplifier is operating in push-pull.

## ACKNOWLEDGMENTS

The author would like to thank all at Toshiba Research Europe Limited for their support in this work, particularly Konstantinos Mimis for producing the PCB.

## REFERENCES

1. Seo, M., Kim, K., Kim, M., Kim, H., Jeon, J., Sim, J., Park, M., Yang, Y., 'Design of a 40 Watt ultra-broadband linear power amplifier using LDMOSFETs', Proceedings of the 2010 Asia-Pacific Microwave Conference, 2010, pp. 414-417.
2. Jain, A., Hannurkar, P.R., Sharma, D.K., Gupta, A.K., Tiwari, A.K., Lad, M., Kumar, R., Gupta, P. D., Pathak, S. K., 'Design and characterization of 50 kW solid-state RF amplifier', International Journal of Microwave and Wireless Technologies, 2012, 4, (6), pp. 595-603.
3. FitzPatrick, D., "Modelling of a Printed VHF Balun Using E-M Simulation Techniques" ARMMS Conference, April 2013, pp. 1-6.
4. Werner, K. 'RF energy systems: realizing new applications', Microwave Journal, 2015, 58, (12), pp. 22-34.

5. Sawdai, D., Pavlidis, D., 'Push-pull circuits using n-p-n and p-n-p InP-based HBT's for power amplification', IEEE Transactions on Microwave Theory and Techniques, 1999, 47 (8), pp. 1439-1448.
6. Watkins, G.T., 'High bandwidth class B totem pole power amplifier for envelope modulators', IET Electronics Letters, 49, (2), 2013, pp. 127-129.
7. Tozawa, Y., 'Design of low-distortion HF transmitter with power MOSFETs', Fifth International Conference on HF Radio Systems and Techniques, 1991, pp. 316-320.
8. Meyer, R.G., Mack, W.D., 'A wide-band class AB monolithic power amplifier', IEEE Journal of Solid-State Circuits, 1989, 24, (1), pp. 7-12.
9. Watkins, G. T., 'A Single Input Transformer-less Push-Pull Microwave Power Amplifier', 2016 IEEE MTT-S International Microwave Symposium Digest (MTT), May 2016, pp. 1-4.
10. Alomar, W., Mortazawi, A., 'A high voltage high power (HiVP) class E power amplifier at VHF', 2011 IEEE MTT-S International Microwave Symposium Digest (MTT), June 2011, pp. 1-4.
11. Whitaker, J. C. The Electronics Handbook, CRC Press, IEEE Press, 1996.
12. Mini-Circuits, 'Computing thermal resistance of PCB-mounted MMIC devices', Microwave Journal, Apr. 2016, pp. 176-180.